Dark resonances with variable Doppler sensitivity

Christian Bolkart, Danijela Rostohar, and Martin Weitz
Physikalisches Institut, Auf der Morgenstelle 14, 72076 Tübingen, Germany

We have studied dark resonances in a thermal gas of rubidium atoms using a variable angle between the two driving optical beams. The inclined angle was tuned between a Doppler-free situation (i.e., collinear beams) and near 10^{-3} rad, yielding an effective Doppler sensitivity of a far-infrared photon. For the case of buffer gas cells, Dicke narrowing occurs. We can carefully control the transition between the Dicke regime, in which the Doppler broadening is suppressed, and the Doppler-broadened regime, in which the thermal atomic motion strongly couples to the three-level atoms.

PACS number(s): 42.50.Gy, 32.70.−n, 42.25.Bs

An optical dense gas of three-level atoms can become transparent if quantum-mechanical interference effects suppress the absorption of a bichromatic optical field [1,2]. The atoms then decouple from the light field and are trapped in a "dark" coherent superposition of ground states. This trapping of states is a resonance phenomenon. The long coherence times available in buffer gas cells have allowed for the observation of dark resonances with spectral linewidths down to below 30 Hz [3,4]. It was noted that the Dicke effect can suppress the residual Doppler broadening present when two superimposed laser beams with optical frequencies differing by an atomic hyperfine ground-state splitting are used [4]. Studies of the Dicke effect in the optical regime also include the observation of dipole resonance effects in thin gas cells [5,6]. Recently, the physics of dark resonances has gained considerable attraction in the context of studies of slow light, which is a benefit of the interesting dispersion properties associated with the spectrally sharp variations in absorption [7]. Moreover, schemes for quantum computation were proposed [8]. While in the context of precision spectroscopy one is usually interested in avoiding the Doppler effect by using collinear beams, dark states have also been investigated in the Doppler-sensitive mode (i.e., with counterpropagating beams), which has, e.g., allowed for the development of novel techniques for laser cooling [9] and atom interferometry [10].

We here report a study of the transition region between Doppler-free and Doppler-sensitive dark resonances. Using rubidium atoms in gas cells both with and without buffer gas, we recorded dark resonances for a variable angle between the two driving laser beams. While the Doppler effect is completely suppressed for a collinear excitation geometry, a small Doppler sensitivity is introduced when the angle between the beams is increased up to typically 10^{-3} rad, which in our setup can be performed in a very controlled way. In this way, the effective photon wavelength is varied between infinity and the millimeter regime. In contrast to the case of a two-level system, the atomic response for the dark-resonance case is not given by the Fourier transform of the driving field. The experimentally observed results are compared with the predictions of a simple analytical model. For spectra recorded with buffer gas cells, the Dicke effect considerably reduces the Doppler sensitivity [11]. Due to frequent elastic collisions, the Doppler effect in the atomic

frame here leads to a continuous spectrum. The thermal motion thus acts as a noise source, whose coupling to the internal atomic states can be adjusted by the angle in a controlled way. We wish to point out that the thermal fluctuations couple to all atoms individually, which cannot be achieved when, e.g., introducing noise to the laser difference frequency. Such studies can, e.g., be of interest in the context of quantum phase transitions of the coupled atom-light system. In recent work, we discussed the possibility of a phase transition between a Bose-Einstein condensate of dark-state polaritons and a thermal, BCS-like state [12], which clearly does require a thermal equilibrium situation. Evidence for a phase transition of quasiparticles to a Bose-Einstein condensate has recently been obtained for excitons [13]. In the present experiment, clearly no thermal equilibrium is yet achieved between atomic and photonic degrees of freedom. On the other hand, also nonequilibrium situations are of current theoretical interest. Our experiment is moreover of interest in the context of decoherence studies of quantum-logic schemes, as it gives limits to the experimentally required beam-pointing accuracies [8].

A level scheme for the observation of dark resonances is shown in Fig. 1. A three-level atom with two stable ground states $|g_+\rangle$ and $|g_-\rangle$ and a spontaneously decaying state $|e\rangle$ is irradiated by two beams of optical frequencies ω_+ and ω_-, where Ω_+ and Ω_- denote the corresponding Rabi frequencies. Let $\hbar\omega_z$ denote the energy splitting between the ground states and $\delta = \omega_+ - \omega_- - \omega_z$ the two-photon detuning. If $\delta = 0$, the coherent "dark" superposition $|\psi_{NC}\rangle = (1/\sqrt{\Omega_+^2 + \Omega_-^2}) \times (\Omega_+|g_-\rangle - \Omega_-|g_+\rangle)$ does not couple to the excited state, and is therefore a stationary eigenstate. This dark state becomes nonstationary for a nonzero two-photon detuning. In this case the dark state couples to the excited state, resulting in a loss rate for the probability of an atom to be in this state. In the Schrödinger picture, this rate is in the case $\Omega_+ = \Omega_-$ $(\equiv \Omega_0/\sqrt{2})$, vanishing one-photon detuning ($\Delta = 0$), and for $\Omega_0 \ll \Gamma$ (where Γ denotes the upper state decay rate) approximately given by [14]

$$\Gamma'_{NC}(\delta) = \frac{\delta^2}{\Omega_0^2}\Gamma. \qquad (1)$$

For the following treatment, assume that spontaneous decay only negligibly repopulates the dark state; as is best realized
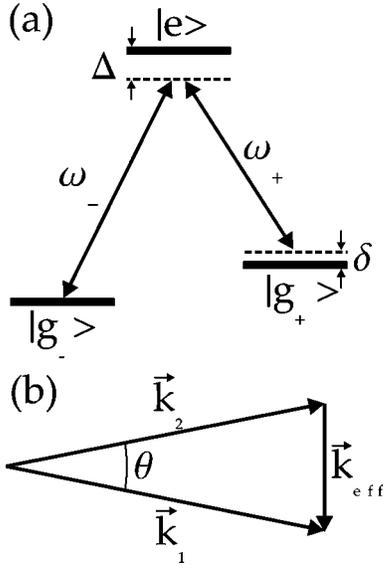
FIG. 1. (a) Schematic representation of the used level scheme and (b) geometry of relevant optical wave vectors.

with an "open" three-level system, where spontaneous decay from $|e\rangle$ mostly populates ground states other than $|g_+\rangle$ and $|g_-\rangle$ (i.e., other hyperfine or Zeeman ground states). Once the atom enters the interaction region, the initial atomic population is projected onto the dark state. For an interaction with constant Rabi frequency, the number of atoms remaining in the dark state after an interaction time T_{ww} is in this model straightforwardly found to be

$$P_{\text{survive}}(\delta) = \exp[-\Gamma'_{NC}(\delta)T_{ww}] = \exp\left(-\frac{\delta^2}{\Omega_0^2}\Gamma T_{ww}\right). \quad (2)$$

For this Doppler-free case, we obtain a Gaussian line shape with a full width at half maximum (FWHM) of

$$\Delta\omega_0 = 2\Omega_0\sqrt{\ln 2/(\Gamma T_{ww})}. \quad (3)$$

The response to a more complex pulse envelope (as seen in the atomic frame) can be derived by temporal integration of the decay rate. In our experiment, the interaction time is time-of-flight limited and of order $d/\bar{v}$ for no buffer gas and d^2/D for a buffer gas cell, respectively, where d denotes the diameter of the laser beam, $\bar{v}$ the mean atomic velocity of the thermal gas, and D the diffusion constant of rubidium atoms in the presence of the buffer gas.

Let us next investigate the dark-resonance signal in the Doppler-sensitive case, as can be explored by introducing a nonzero angle θ between the driving laser beams. The Doppler effect modifies the two-photon detuning by an amount $\vec{k}_{\text{eff}} \cdot \vec{v}$, where $\vec{v}$ denotes the atomic velocity and $\vec{k}_{\text{eff}} = \vec{k}_+ - \vec{k}_-$ the effective wave vector of the two-photon transition [see also Fig. 1(b)]. For $\theta \ll 1$, the Doppler shift can be written as $\Delta\omega_D \approx 2kv_x\theta$ (where $\vec{k}_+ \approx -\vec{k}_- \approx \vec{k}$, if we assume that $\vec{k}_{\text{eff}}$ is directed along the x axis).

We shall now consider an atomic distribution, and first give the exact formula for the average probability of atoms remaining in the dark state for the case of no buffer gas

$$\bar{P}_{\text{survive}} = \int d^3x_0 \int d^3v\rho(\vec{x}_0,\vec{v})\exp\left[-\int dt\,\Gamma\frac{(\delta-\vec{k}_{\text{eff}}\cdot\vec{v})^2}{\Omega_0^2(\vec{x}_0+\vec{v}t)}\right], \quad (4)$$

,where $\rho(\vec{x}_0,\vec{v})$ denotes the probability for an atom to have a velocity $\vec{v}$ and be located at position $\vec{x}_0$ at $t=0$ $[\vec{x}(t=0)=\vec{x}_0]$, which fully incorporates the time-dependent Rabi frequency experienced during the passage through the laser beam.

The complexity of the problem is considerably reduced if we assume a constant Rabi frequency for all atoms, which is experienced for a fixed (average) interaction time T_{ww}. We then are left with the much simpler inhomogeneous line shape $\bar{P}_{\text{survive}} \approx \int dv_x f(v_x)\exp\{-[(\delta-k_{\text{eff}}v_x)^2/\Omega_0^2]\Gamma T_{ww}\}$, where $f(v_x)$ denotes the atomic velocity distribution along the x axis. For a Maxwellian velocity distribution $f(v_x) \propto e^{(-v_x/v_w)^2}$ the line shape is the convolution of two Gaussian curves, which again yields a Gaussian total line profile of FWHM $\Delta\omega_{\text{tot}} = \sqrt{\Delta\omega_0^2 + \Delta\omega_D^2}$. When no buffer gas is present, the additional broadening is

$$\Delta\omega_D = 2kv_x \cdot 0 = 4\sqrt{\ln 2}kv_w\theta, \quad (5)$$

where $v_w = \sqrt{2kT/m}$ denotes the most probable atomic velocity [15].

In the buffer gas cell, the atoms undergo frequent velocity-changing collisions, which results in a Doppler shift varying rapidly with time. The resulting physics is more conveniently analyzed in the frequency domain. If the mean free path is smaller then the effective wavelength $\lambda_{\text{eff}}(\theta) = \lambda/2\pi\theta$, the Doppler effect is suppressed and Dicke narrowing occurs [11]. Our experimental setup allows for an elegant adjustment of λ_{eff}. In the atomic frame, the two-photon optical field has a Lorentzian spectrum of frequency width [which follows from Dicke's formulas when λ is replaced by $\lambda_{\text{eff}}(\theta)$]

$$\Delta\omega_{D,\text{buffer}}(\theta) = \frac{8\pi^2D}{\lambda_{\text{eff}}^2} = \frac{32\pi^2D}{\lambda^2}\theta^2. \quad (6)$$

Since the atomic response of the three-level atoms is not directly a Fourier transform of the driving fields, the physics is different from that in the original treatment of Dicke. At present we do not have a full model for the line shape of the homogeneously broadened spectra with buffer gas. We expect that the total linewidth of the spectrum will be of order $\Delta\omega_{\text{tot,buffer}} = \sqrt{\Delta\omega_0^2 + \Delta\omega_{D,\text{buffer}}^2}$ [16].

Our experimental setup is schematically shown in Fig. 2. Two optical beams derived from the diode laser (locked to the $F=2 \rightarrow F'=1$ hyperfine component of the $D1$ line in ^{87}Rb) each double pass an acousto-optic modulator. Subsequently the beams are spatially filtered with 30-μm-diameter pinholes. The orthogonally polarized beams are recombined with a polarizing beam splitter, and then pass a further, removable pinhole of 50 μm diameter (RPH in Fig. 2), which is used for alignment purposes only. Subsequently, a lens of $f=300$ mm focal length collimates the optical beams to a 5.56 mm diameter. The beams then are converted into orthogonal circular polarizations with a $\lambda/4$ plate and sent through a heated rubidium cell. During the alignment proce-
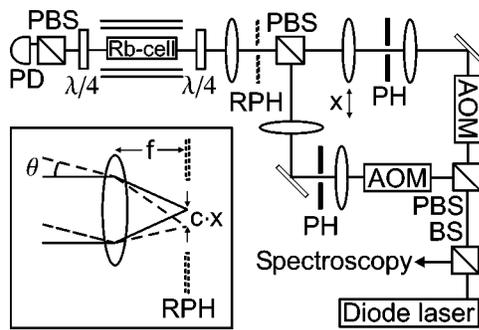
FIG. 2. Simplified schematic of the experimental setup. The angle θ between the two driving laser beams was adjusted by horizontal movement of the lens before the laser beams were merged. The introduced angle variation from this movement can be easily estimated from the position displacement achieved in the focal plane of the removable pinhole (RPH; see drawing in the inset). PD, photodiode; PBS, polarizing beam splitter; AOM, acousto-optic modulator; PH, pinhole; BS, beam splitter.

dure, the removable pinhole (RPH in Fig. 2) is added into the beam paths, which allows us to reduce the angle between the two driving beams passing through the cell (i.e., in the Fourier plane of the pinhole, as indicated in the inset of Fig. 2) to below an estimated value of 10^{-5} rad. After the adjustment procedure, the pinhole is removed. With no spatial translation of the lens, the two driving optical beams remain precisely copropagating and Doppler-free spectra can be recorded. By transversally displacing the lens located before the recombining beam splitter with a micrometer translation stage (see Fig. 2), the position of the focus of this beam in the RPH plane is transversally shifted, which results in a nonzero angle θ between the collimated beams passing the rubidium cell. For our experimental geometrical parameters, a typical spatial lens translation of $x=10$ μm results in an angle variation $\theta=(3.1\pm0.1)\times10^{-4}$ rad at the position of the cell. For these parameters, the transversal displacement of the beams is 23 μm, which is roughly two orders below the beam diameter and not expected to affect the experiments.

In a typical experimental run, the rubidium cell is heated to 340 K (corresponding to 2×10^{-5} Torr of rubidium vapor pressure [17]) to increase the optical density. The cell is magnetically shielded with two layers of μ-metal, and within the shielding a homogeneous 40 mG bias field is applied directed longitudinally to the laser beams. The best results are obtained with power ratios near 1:4 and 1:2 of signal and control beams in the cases of buffer gas and no buffer gas, respectively. The data presented here were recorded with 190 μW optical power in the signal and 770 μW in the control beam when the cell with 20 Torr of neon buffer gas was used, while for the spectra without buffer gas 280 μW in the signal and 480 μW in the control beam were applied. The optical difference frequency of the beams is scanned through the two-photon resonance by varying the drive frequency of one of the acousto-optic modulators. Simultaneously, we detect the transmitted intensity of the frequency-modulated, circularly polarized beam through the cell with a photodiode. To allow for a lock-in detection technique, we periodically amplitude-modulate the oppositely polarized optical beam
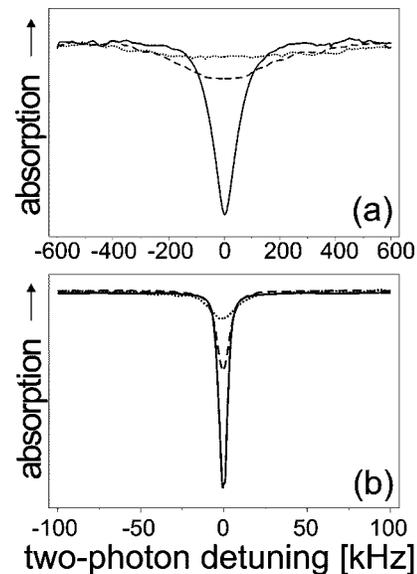

FIG. 3. Rubidium dark-resonance spectra obtained in experiments (a) without and (b) with 20 Torr neon buffer gas. Note the different frequency scales for the two classes of spectra. The measurements were recorded for no angle between the driving beams (solid line), and angles of $\theta=(3.08\pm0.1)\times10^{-4}$ (dashed line), and $(6.15\pm0.1)\times10^{-4}$ (dotted line) rad.

and phase-sensitively detect the photodiode signal.

Typical experimental spectra are shown in Fig. 3(a) for no buffer gas, and Fig. 3(b) for 20 Torr neon buffer gas for three different angles between laser beams. The spectra have been fitted with Gaussian line profiles. For collinear beams, the linewidth is 100 kHz with no buffer gas, which reduces to 5.8 kHz for the case of buffer gas due to the much larger interaction time in the latter case. If we introduce a finite angle between the two driving optical beams, the amplitude of the dark resonances decreases and the linewidth increases. While for a zero angle between the beams the effective wavelength of a two-photon transition is infinite, it reduces to $\lambda_{\text{eff}}=2\pi/k_{\text{eff}}\approx0.67$ mm for an angle of 6×10^{-4} rad. Clearly, the product $k_{\text{eff}}d$ (corresponding to the Lamb-Dicke factor) here exceeds unity, from which it becomes clear that at least in the absence of buffer gas we have to consider the Doppler effect. In the frequency domain, the Doppler broadening in this case exceeds the time-of-flight broadening (for $k_{\text{eff}}v\gtrsim v/d$). We find that the amplitude of the dark resonance is close to the Doppler-free case as long as the Doppler effect does not contribute significantly to the linewidth, but decreases rapidly for larger angles. For the case with buffer gas, the Dicke effect, despite the narrower Doppler-free width, reduces the Doppler sensitivity when the effective wavelength of the two-photon transition becomes comparable to the mean free path. Figure 4 gives measured parameters for a series of spectra as a function of the inclined angle between the beams for both (a) without and (b) with buffer gas. The top row of Fig. 4 shows the variation of the observed linewidth (dots) as a function of the angle between the beams fitted with our theoretical model. For the buffer gas spectra, a much slower increase in Doppler width is observed for small angles, which is well understood in terms of
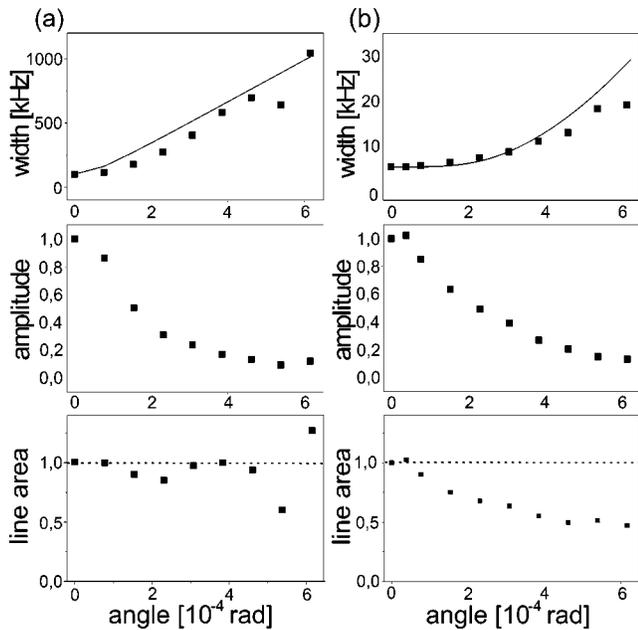
FIG. 4. Linewidth (top row), relative line amplitude (middle row), and relative line area (bottom row) of dark-resonance spectra as a function of angle between the driving optical beams (a) without and (b) with buffer gas. The experimental results (dots) have been fitted with the results of our simple model (solid line) in (a) and (b) in the top row [where we used $\Delta\omega_{\text{tot}} = \sqrt{\Delta\omega_0^2 + \Delta\omega_D^2}$ with Eqs. (3) and (5) for (a) and $\Delta\omega_{\text{tot,buffer}} = \sqrt{\Delta\omega_0^2 + \Delta\omega_{D,\text{buffer}}^2}$ with Eqs. (3) and (6) for (b)]. The dashed lines in the graphs in the bottom row at constant line area give in our model the expected dependence for the case without buffer gas (a), while no model is available yet for the case with buffer gas (b).

the expected quadratic dependence of the Doppler width on angle variations. The middle and bottom rows of Fig. 4 show the dependence of the observed resonance amplitude and the line area as a function of the angle between the beams. For the case with no buffer gas, our model predicts that the line area is independent of angle (from which also the amplitude follows). This is approximately satisfied for the experimental spectra. We do not have a model for the case with buffer gas yet, for which one would have to study the response of dark resonances to multifrequency fields. One experimentally observes that the line area for the largest used angles (6 $\times 10^{-4}$ rad) reduces to roughly one-half of that of the Doppler-free case. We attribute this decrease as related to the here inhomogeneous nature of the Doppler broadening. For larger angles between the beams, all atoms in their rest frame experience Fourier components of high Raman difference frequency, which leads to an increase of the depumping rate of the dark state.

To conclude, we report a study of the transition regime between Doppler-free and Doppler-sensitive dark resonances, where the effective wavelength is varied from infinity to the millimeter regime. For the future, it would be important to develop a refined theoretical model studying the dark-resonance response both with and without buffer gas.

[1] G. Alzetta, A. Gozzini, L. Moi, and G. Orriols, Nuovo Cimento Soc. Ital. Fis., B **36**, 5 (1976).
[2] See, e.g., E. Arimondo, Prog. Opt. **35**, 257 (1996).
[3] R. Wynands and A. Nagel, Appl. Phys. B: Lasers Opt. **68**, 1 (1995); S. Brandt, A. Nagel, R. Wynands, and D. Meschede, Phys. Rev. A **56**, R1063 (1997).
[4] M. Erhard and H. Helm, Phys. Rev. A **62**, R061802 (2000).
[5] G. Dutier, A. Yarovitski, S. Saltier, A. Papoyan, D. Sarkisyan, D. Bloch, and M. Ducloy, Europhys. Lett. **63**, 35 (2003).
[6] D. Sarkisyan, T. Varzhapetyan, A. Sarkisyan, Yu. Malakyan, A. Papoyan, A. Lezama, D. Bloch, and M. Ducloy, Phys. Rev. A **69**, 065802 (2004).
[7] L. V. Hau et al., Nature (London) **397**, 594 (1999); Kash et al., Phys. Rev. Lett. **82**, 5229 (1999).
[8] M. D. Lukin, S. F. Yelin, and M. Fleischhauer, Phys. Rev. Lett. **84**, 4232 (2000).
[9] A. Aspect, E. Arimondo, R. Kaiser, N. Vansteenkiste, and C. Cohen-Tannoudji, Phys. Rev. Lett. **61**, 826 (1988).
[10] M. Weitz, B. C. Young, and S. Chu, Phys. Rev. Lett. **73**, 2563 (1994).
[11] R. H. Dicke, Phys. Rev. **89**, 472 (1953).
[12] C. Bolkart, R. Weiss, D. Rostohar, and M. Weitz, Laser Phys. **15**, 3 (2005); C. Bolkart et al. (unpublished).
[13] L. V. Butov, A. C. Gossard, and D. S. Chemla, Nature (London) **418**, 751 (2002); see also the critical discussion by

C. W. Lai et al., Science **303**, 503 (2004)
[14] This formula can be derived when adiabatically eliminating the excited- and coupled-state amplitudes. It also follows from Eq. 11.26b [which states $\Gamma'_{NC}(p) = (4k^2p^2)/(m^2\Omega_1^2)\Gamma$] in C. Cohen-Tannoudji, in *Fundamental Systems in Quantum Optics*, edited by J.Dalibard, J.-M.Raimond, and J.Zinn-Justin, Proceedings of the Les Houches Summer School of Theoretical Physics, LIII, 1990 (Elsevier, Amsterdam, 1992), where Doppler-sensitive dark resonances are considered. In this formula p denotes the atomic momentum, m the atomic mass, Γ the departure rate from the excited state, and the Ω_1 ($\equiv\Omega_0$) the Rabi frequency. Our formula is obtained by replacing the two-photon Doppler shift $2kp/m$ by the two-photon detuning δ.
[15] See, e.g., W. Demtröder, *Laser Spectroscopy* (Springer-Verlag, Berlin, 1996).
[16] Note that the response of the three-level atom in its rest frame to the two-photon optical field with Lorentzian line shape does not necessarily yield a Lorentzian form of the atomic response. Given this issue, we have for an estimation of the total linewidth of the buffer gas spectrum given the quoted simple formula which is strictly valid only for the convolution of two Gaussians.
[17] See, e.g., D. A. Steck, rubidium (^{87}Rb) D line data, available at http://steck.us/alkalidata